An all-metallic logic gate based on current-driven domain wall motion

PENG XU, KE XIA*, CHANGZHI GU*, LING TANG, HAIFANG YANG AND JUNJIE LI

Beijing National Laboratory for Condensed Matter Physics, Institute of Physics, Chinese Academy of Sciences, Beijing 100080, China
***e-mail: czgu@aphy.iphy.ac.cn**

Published online: 3 February 2008; doi:10.1038/nnano.2008.1

The walls of magnetic domains can become trapped in a ferromagnetic metallic point contact when the thickness of the film and the width of the contact are less than their critical values[1]. The discovery that domain walls can be moved from such constrictions by a sufficiently large current has attracted considerable attention from researchers working on both fundamental research and potential applications[2–12]. Here we show that Invar nanocontacts fabricated on silica substrates exhibit a sharp drop in resistance with increasing bias voltage at room temperature in the absence of an applied magnetic field. Moreover, when two nanocontacts are combined in an all-metallic comparison circuit, it is possible to perform logical NOT operations. The use of electrical currents rather than applied magnetic fields to control the domain walls also reduces energy consumption and the risk of crosstalk in devices[13,14].

We fabricated nanocontact structures on an Invar alloy film using electron beam lithography (EBL) and the lift-off technique. First, EBL was used to precisely define the nanocontact structure and radio-frequency magnetic sputtering was used to deposit a 30-nm-thick layer of Invar alloy and a 2-nm-thick cap layer of Au. Ultrasonic assisted lift-off in acetone was carried out to obtain the wire and nanocontact. A second EBL process was carried out to define the electrical measurement pads. Figure 1 shows scanning electron microscope (SEM) images of the contact point with a 100-nm-wide contact (Fig. 1a) and the geometry of the measurement pads (Fig. 1b). Finally, a four-probe direct current (d.c.) measurement system was bonded to the pads with Au wire, which were located 5 μm apart and centred on the contact. A Keithley 6485 and 2182A d.c. system was used to take measurements at room temperature without any applied magnetic field. All measurements were carried out after reversal from saturation.

Figure 2 shows a plot of resistance versus voltage for the sample shown in Fig. 1. A sharp drop in resistance was observed as the voltage exceeded a critical value, corresponding to the change in the magnetization configuration of a nanocontact before and after the current density in it reached a critical value. Many reports have shown that a nanocontact structure could pin a domain wall as a defect due to spontaneous magnetization[1,12]. The difference between the two resistance states in the nanocontact structure can be attributed to the removal of the domain wall (DW) from the nanocontact by the reflection of spin-polarized electrons. The resistance of the structure is dominated by the contact position, and electrons experience a spin-dependent reflection at the contact. When a current passes through the DW, a spin-polarized incident electron current will exchange angular momentum with the local magnetic moment of the DW (ref. 12), which applies pressure on the DW. As the current density increases, the DW is pushed away from the contact position and the resistance of the contact decreases. Further measurements with regard to hysteresis revealed that the resistance jumps back when the voltage decreases below the critical value, as shown in Fig. 2. This feature has the potential to be very useful for signal feedback in circuit applications. From the above results, we can conclude that the resistance state can be controlled by the current density, which behaves as a 'write' function in a logical circuit.

Based on our understanding of the properties of DWs in nanocontacts as described above, we were able to fabricate a nanocontact structure in which it was possible to control the resistance change due to DW motion, allowing the two different resistance states to be exploited in logic applications. An all-metallic circuit was designed and fabricated, using the same technique, incorporating two nanocontact structures and two pieces of necked wire. Invar alloy necked wire of appropriate length was used as a comparison resistance so that the resistance drop in the nanocontact could be effectively converted to a voltage signal. By driving an electrical input signal into this circuit, it could function as a NOT gate and output an electrical signal.

A NOT gate, or inverter, is a basic logic element that converts a logic 0 into a logic 1, and a logic 1 into a logic 0. Our NOT gate circuit was constructed from two metal nanocontacts and nanowires incorporated into a 'comparison circuit'. Figure 3a shows the SEM image of the all-metallic logic gate. Two identical 50-nm-wide nanocontacts were fabricated, each in series with a 400-nm-wide wire, and then one nanocontact/wire combination connected in an anti-parallel arrangement with the other. The length of the wire was chosen so that the resistance of the wire approximated that of the nanocontact resistance in its low resistance state. First, the supply voltage had to be properly selected and applied between A and B, as shown in Fig. 3a, to ensure that the current density through both nanocontacts was just below that necessary to switch the resistance state of the nanocontact structures. When the input voltage $V_{input} = 0.1$ V was applied between C and D, the current density in the nanocontacts exceeded the critical value and the DW was pushed away from the nanocontacts, setting the contacts to the low resistance state, which now just matched the resistance in each

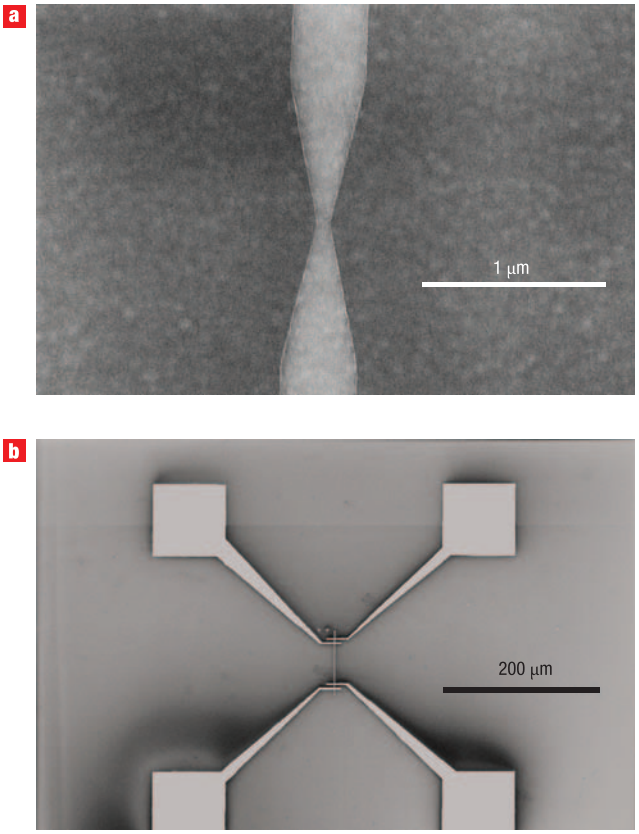

Figure 1 Scanning electron microscope (SEM) images of Invar circuits on silica substrates. a, The nanocontact is ~100 nm wide and 30 nm thick, and is capped with a 2-nm layer of gold to prevent oxidation. **b**, Four-probe DC measurements help to avoid errors arising from the contact resistance between the gold pads (which are about 100 nm thick) and the sample. The *I*–*V* measurements were performed by sweeping the applied voltage from 0 V to 1 V in steps of 5 μV. All measurements were carried out at room temperature and with no applied magnetic field.

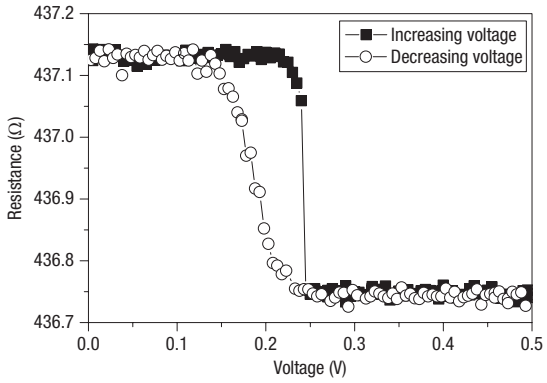

Figure 2 Direct current measurements showing the switching action. There is a sharp drop in resistance when the voltage exceeds a critical value. When the voltage is reduced below the critical value, the resistance returns to its original value less rapidly.

wire. As a result, the resistances in all arms of the circuit were effectively the same, so the potential differenence between E and F was zero. When the input voltage, V_{input}, was set to 0 V, the contact resistance remained in the high resistance state, setting $V_{output} = 0.21$ mV. This output voltage should make a rapid transition from one logic level to the other when the input logic level is changed. Therefore, we assigned logic 0 to the low voltage state of V_{input} and V_{output}, and logic 1 to their high voltage states. According to this definition and the changing voltage levels of V_{input} and V_{output}, this circuit can function as a NOT gate. We acquired the data in Fig. 3b over 60 min of cycling. This corresponds to the circuit undergoing 1,200 NOT operations. All of these NOT operations were performed properly and stably, which demonstrates that the operation of our device is reproducible and reliable. Furthermore, Fig. 3c shows that the output voltage can make a rapid transition from one logic level to the other as the input voltage is swept. With the input voltage starting at 0 V, the output voltage first holds its level, then becomes immeasurably low with increasing input voltage. This indicates the motion of the DW from in the nanocontact to out.

Because the magnetoconstriction of Invar alloy is such that it can compensate for its own thermal deformation, the length of the wires used in this experiment changed by such a small amount that their resistance remained stable, and matched the required value throughout the measurements. Our nanocontact circuit retained its stability after operating over many cycles, and its run-to-run reliability was 100%. The two series contact-and-wire arrangements have DW motion in one direction only. It is essential for operation that this fully flexible magnetic logic architecture be able to return the DW to the contact position, that is, the high resistance state of the contact.

The main logic function of this circuit is reliant on the motion of the DW, so the computing speed of the circuit is determined by the intrinsic oscillation frequency of the DW. We used a new measurement method[8,15] to explore the current-driven DW motion by applying a high-frequency (0–10 MHz) alternating current (a.c.). We succeeded in pinning a single DW in a nanocontact. An a.c. voltage near the critical intensity was applied to both sides of the contact. The current intensity measurements of the a.c. showed the energy absorption of the single DW.

The resonances of the DW with different contact widths are shown in Fig. 4a. Figure 4b shows a decrease in resonance frequency as the width of the DW increases. The energy should be absorbed when the electric-field frequency matches the intrinsic oscillation frequency of the DW. The DW mass is theoretically given by[15,16]

$$m = h^2 N/(4\pi^2 K W^2),$$

where h, N, K and W are Plank's constant, the number of spins in the DW (which is proportional to DW volume), the transverse-magnetic anisotropy energy and the DW width. As the DW thickness is linearly dependent on the DW width, the resonance frequency decreases with the width of the DW as $f \approx 1/W^{1/2}$ according to the frequency–mass relation $f^2 = k/m$ for small oscillations, where k is the elastic constant—this fits our experimental data well (see Fig. 4b).

From Fig. 4 we can see that the maximum computing speed for this circuit could be controlled by controlling the width of the nanocontacts. For example, the intrinsic oscillation frequency of a 50-nm nanocontact is 7.5 ± 0.1 MHz, thus the NOT circuit made from two 50-nm nanocontacts could reach the maximum logic computing speed of 7.5 ± 0.1 MHz. That would halve if the synchronousness of motion of the two DWs were considered.

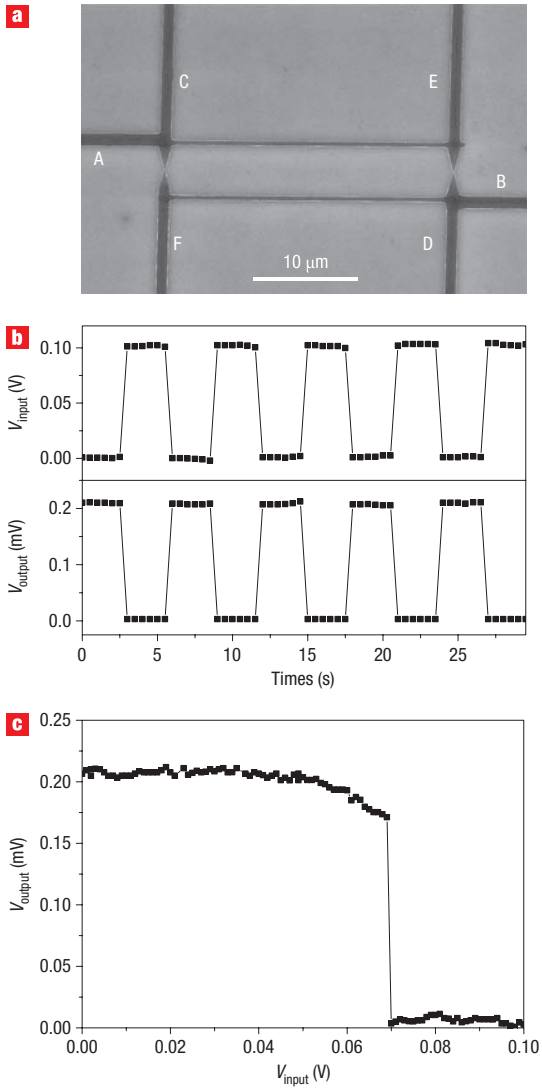

Figure 3 Logic NOT gate circuit and testing results. a, SEM image of the logical NOT circuit, which contains two identical 50-nm-wide nanocontacts (the narrow points in the two dark vertically arranged structures), connected by two 400-nm-wide wires (dark horizontal structures). Both nanocontacts and wires are made from Invar. **b**, Input and output voltages as a function of time. The supply voltage was applied between A and B (see panel **a**), the input voltage (top) was applied between C and D, and the output voltage was measured between E and F. The logical NOT operation can be clearly seen. **c**, Output voltage as a function of the input voltage.

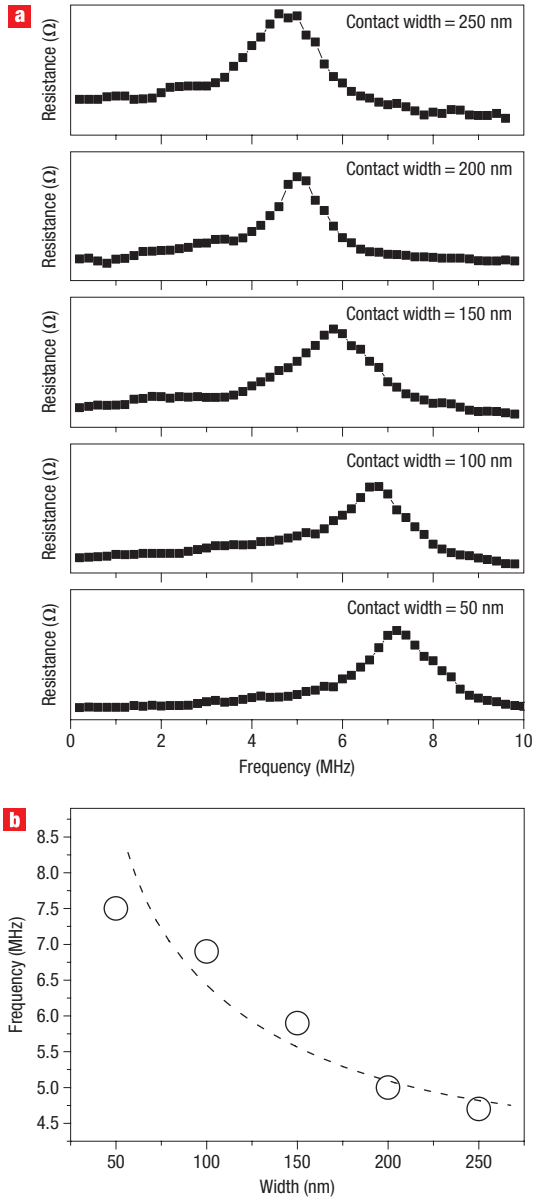

Figure 4 Width effects in the a.c. resistance spectra. a, Frequency spectra for various contact widths: the peak occurs at the resonance frequency of the single DW, where the energy absorption is highest. **b**, The resonance frequency f increases as the width W is reduced. As explained in the text, the data can be approximated using the relation $f \approx 1/W^{1/2}$ (dashed curve).

Because electric energy is consumed by thermal dissipation in this circuit, the power dissipation could be estimated using the relation $P = VI = 1.2 \times 10^{-4}$ W (where $V = 0.24$ V and $I = 5.1 \times 10^{-4}$ A, obtained from experimental data), which is very low compared with that of a Si circuit.

In summary, we have performed a logical NOT operation in an all-metallic circuit at room temperature without the use of an applied magnetic field. Moreover, the high carrier densities made possible by the use of metals rather than semiconductors, the fact that electrical controls should make it relatively straightforward to communicate with standard CMOS circuitry, and the relative simplicity of the circuits (multilayer heterostructures are not involved) should also make it possible to scale the circuits to smaller sizes.

Received 13 November 2007; accepted 21 December 2007; published 3 February 2008.

References

1. Lepadatu, S., Xu, Y. B. & Ahmad, E. Current induced magnetic switching in $Ni_{80}Fe_{20}$, Ni, Fe, and Co wires. *J. Appl. Phys.* **97,** 10C711 (2005).
2. Yamaguchi, A. *et al.* Real-space observation of current-driven domain wall motion in submicron magnetic wires. *Phys. Rev. Lett.* **92,** 077205 (2004).
3. Lepadatu, S. & Xu, Y. B. Direct observation of domain wall scattering in patterned $Ni_{80}Fe_{20}$ and Ni nanowires by current–voltage measurements. *Phys. Rev. Lett.* **92,** 127201 (2004).

4. Bagrets, A., Papanikolaou, N. & Mertig, I. Magnetoresistance of atomic-sized contacts: An *ab initio* study. *Phys. Rev. B* **70,** 064410 (2004).
5. Yamanouchi, M., Chiba, D., Matsukura, F. & Ohno, H. Current-induced domain-wall switching in a ferromagnetic semiconductor structure. *Nature* **428,** 539–542 (2004).
6. Labaye, Y., Berger, L. & Coey, J. M. D. Domain walls in ferromagnetic nanoconstriction. *J. Appl. Phys.* **91,** 5341–5346 (2002).
7. Ono, T. *et al*. Propagation of a magnetic domain wall in a submicrometer magnetic wire. *Science* **284,** 468–470 (1999).
8. Thomas, L. *et al*. Oscillatory dependence of current-driven magnetic domain wall motion on current pulse length. *Nature* **443,** 197–200 (2006).
9. Laufenberg, M. *et al*. Temperature dependence of the spin torque effect in current-induced domain wall motion. *Phys. Rev. Lett.* **97,** 046602 (2006).
10. Ohe, J. & Kramer, B. Dynamics of a domain wall and spin-wave excitations driven by a mesoscopic current. *Phys. Rev. Lett.* **96,** 027204 (2006).
11. Beach, G. S. D., Knutson, C., Nistor, C., Tsoi, M. & Erskine, J. L. Nonlinear domain-wall velocity enhancement by spin-polarized electric current. *Phys. Rev. Lett.* **97,** 057203 (2006).
12. Versluijs, J. J., Bari, M. A. & Coey, J. M. D. Magnetoresistance of half-metallic oxide nanocontacts. *Phys. Rev. Lett.* **87,** 026601 (2001).
13. Allwood, D. A. *et al*. Submicrometer ferromagnetic NOT gate and shift register. *Science* **296,** 2003–2006 (2003).
14. Allwood, D. A. *et al*. Magnetic domain-wall logic. *Science* **309,** 1688–1692 (2005).
15. Saitoh, E., Miyajima, H., Yamaoka, T. & Tatara, G. Current-induced resonance and mass determination of a single magnetic domain wall. *Nature* **432,** 203–206 (2004).
16. Tatara, G. & Kohno, H. Theory of current-driven domain wall motion: spin transfer versus momentum transfer. *Phys. Rev. Lett.* **92,** 086601 (2004).

Acknowledgements

We wish to thank Dongmin Chen, Enge Wang and Zheng Cui for fruitful discussions. This work was supported by the National Natural Science Foundation of China (grant no.90406024-1), the Ministry of Science and Technology of China (grant nos 2006CB933000 and 2006AA03Z402) and the Knowledge Innovation Program of the Chinese Academy of Sciences (CAS), China.
Correspondence and requests for materials should be addressed to C.G.

Author contributions

C.G. and K.X. conceived and designed the experiments. P.X., H.Y. and J.L. performed the experiments. C.G., K.X., P.X. and L.T. analysed the data. C.G., P.X. and K.X. co-wrote the paper. All authors discussed the results and commented on the manuscript.